THE COSMIC EXPLORER GRAVITATIONAL-WAVE OBSERVATORY

Technical Note	**CE-T2400019-v3**	2024/09/27

The Cosmic Explorer Observatory Coating Requirements and R&D

Stefan Ballmer, Lisa Barsotti, GariLynn Billingsley, Matthew Evans, Martin Fejer, Andri Gretarsson, Gregg Harry, Kevin Kuns, Carmen Menoni, Swadha Pandey, Steve Penn, Stuart Reid

This is an internal working
note of the COSMIC EXPLORER project.

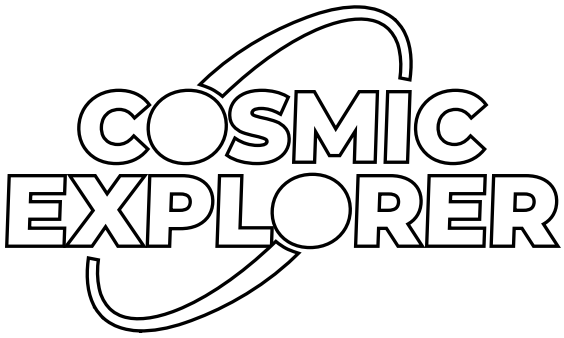

http://www.cosmicexplorer.org/

Contents

1 Overview

Coating thermal noise (CTN) is one of the fundamental noises that limits the sensitivity of gravitational-wave detectors. Research into coating materials with outstanding optical proprieties such as low absorption and low scatter, yet low mechanical loss (and thus low thermal noise), has been a sustained effort throughout the history of the field. The resulting Advanced LIGO coatings are amorphous Ion-Beam Sputtered (IBS) coating layers of titania and tantala (high index material) and silica (low-index material). Direct measurements of the Advanced LIGO CTN have been made on witness samples with small spot size on small optics, and the results are close to what is expected from theory [1]. At the time of the O4 Observing Run, the LIGO Livingston noise budget shows a best fit for a noise with $f^{-0.45}$ shape between about 50 Hz and 200 Hz) and an amplitude spectral density 1.3 times higher than predicted based on the witness sample measurement[1]. For the purpose of this document we will refer to the CTN inferred from these witness sample measurements as "aLIGO CTN" or "aLIGO Witness", though there may be some variation in the thermal noise inferred from direct measurements at the LIGO observatories ("LLO Upper limit").

In addition to CTN, **optical absorption** in the main interferometer optics (a.k.a. "test masses") has been identified as the main hurdle to Advanced LIGO operating at the higher power levels, thus preventing it from realizing the associated lower quantum noise. Optical absorption comes in two flavors that require different mitigation strategies:
(i) **Point absorbers**, i.e. small spots (less than about 100 µm) on the coating with very high absorption. When they absorb on the order of 10 mW, they lead to local heating and deformation of the test masses, this distorts the optical wave front and leads to scattering of optical power[2]. These hot spots develop on a time scale of a few minutes, and are very difficult to correct due to their high spatial frequency (i.e., small size). Investigations on de-installed optics and the coating deposition machines suggest that at least some of those absorbers are due to contamination introduced during the coating process.
(ii) **Uniform background absorption** is typically determined by the material and manufacturing process (as opposed to idiosyncratic particulate contamination). The Advanced LIGO optics achieved absorptions of approximately 0.5 ppm (see Table 2), but this level still would result in about half a Watt of absorbed power at the nominal operating power level. Because the heat is spread out across the whole optic, the time constant of the associated thermal lens is extremely long - Advanced LIGO teat masses take about 12 h to reach thermal equilibrium, and Cosmic Explorer's larger mirrors will increase this time by a factor of about four. Design work is ongoing on ways to mitigate this uniform thermal lensing in a way that avoids lock acquisition transients. However, a reduction of the uniform optical absorption to below 0.1 ppm would significantly simplify Cosmic Explorer operations. Moreover, demonstrating the feasibility of such low-absorption coatings would simplify the optical design of Cosmic Explorer. These coatings would also find applications in other research fields, ranging from precision measurement to high power applications such as laser fusion [3].

[1] See https://alog.ligo-la.caltech.edu/aLOG/index.php?callRep=70274, with investigations ongoing to understand the origin of the excess of noise

An ongoing international research effort led in the US by the Center for Coatings research aims to deliver a coating technology for the LIGO A+ detectors with a CTN amplitude spectral density (ASD) which is a factor of 2 below the aLIGO CTN. While target has not yet been achieved, the best coatings to date showing an improvement of 0.6 times the aLIGO CTN (still in ASD), based on measurements in samples, with some optical proprieties still to be fully analyzed. Optimizing the design of a coating based on this technology may produce CTN levels that approach the factor of 2 goal. Here we will refer to this goal as "A+ CTN" (i.e. "A+ CTN" = 0.5×"aLIGO CTN"). The CE 40 km baseline design [4] assumes that this target will be achieved before CE test masses are coated (i.e., nominally in the mid-2030s).

Recently, the concept for an improved LIGO detector in current facilities, known as A$^\sharp$, has taken form [5]. The A$^\sharp$ concept includes coatings which are another factor of 2 better than the A+ target, i.e. "A$^\sharp$ CTN" = 0.25×"aLIGO CTN" (in ASD). To date, only samples made of AlGaAs crystalline coatings have shown such low CTN. However, scaling AlGaAs coatings to the size required for A$^\sharp$ presents a manufacturing challenge, and optical properties such as birefringence and point absorbers remain to be fully characterized [6].

In light of these developments, this note aims to:

- Clarify the impact of coating thermal noise in Cosmic Explorer (CE);
- Clarify the impact of optical coating properties (absorption, birefringence, etc) on CE;
- Compare plausible CE sensitivity targets with different coating designs;
- Summarize plausible R&D paths and decision points.

2 Coating Requirements and Reference Design

2.1 Coating Thermal Noise Scaling

As described in App. A, for a fixed cavity geometry, CTN ASD scales as $L_{\rm arm}^{-3/2}$, while for a fixed spot size CTN ASD scales as $L_{\rm arm}^{-1}$. For this reason, the longer the interferometer arm, the lower the noise – with the caveat that the mirror size needs to increase to accommodate the larger beam spot. This is the fundamental reason why the CE 40 km detector does not need to rely entirely on improved coating designs to boost its sensitivity. Since the CE 40 km detector has approximately twice the spot diameter and ten times the arm length of Advanced LIGO, the CTN ASD is already improved by a factor of ∼20 with respect to existing 4 km detectors (Table 1).

For the 20 km CE detector, we have a choice of matching either the spot size or the cavity geometry to the 40 km detector. With respect to existing 4 km detectors this results in an improvement by a factor of 9.7 (CE 20 km), or 6.9 (CE 20 km min., Table 1).

L_{arm}	beam spot size (w)	test mass radius	CTN ASD scaling
CE 40 km	12 cm	35 cm	19.4
CE 20 km	12 cm	35 cm	9.7
CE 20 km min.	8.5 cm	24.7 cm	6.9
aLIGO	6.2 cm	17 cm	1 (ref)

Table 1: Arm length, spot size, test mass radius and Coating Thermal Noise Amplitude Spectral Density (CTN ASD) scaling with respect to Advanced LIGO (calculated as $[L\,w]/[L\,w]_{\rm aLIGO}$). For the 20 km detector we can either keep the spots as small as diffraction allows (CE 20 km min.), or adjust the g-factor to have the same optic and spot size as the 40 km detector (CE 20 km), depending on the coating availability.

2.2 Detector Considerations

There are other aspects of the detector design that impact requirements on CTN:

- The CE quantum noise can be tuned to either a broadband sensitivity (this is the reference sensitivity curve for CE 40 km), or tuned to maximize binary insprial range, which results in a detector focused on frequencies between 10 Hz and 100 Hz, with a quantum noise a factor of 2 lower in that band (compared to the CE 40 km reference sensitivity). This "low-frequency tuning" would benefit from CTN levels below the "A+ CTN" level.
- The larger test masses and suspensions push the CE observation band to lower frequencies by approximately a factor of 2 compared to Advanced LIGO, thus requiring a slightly lower thermal noise than suggested by the simple scale factors in Table 1.
- A CE 20 km design can change significantly depending on coating availability. If the CTN ASD is reduced below the A$^\sharp$ CTN level (a factor of four below Advanced LIGO CTN), the CE 20 km detector can be built with minimal spot size, reducing the cost for large optics and a large vacuum system diameter. If such a coating is not available,

the CE 20 km detector would likely be designed to have the same size optics as the 40 km detector. (See Table 1.)

2.3 Network Considerations

To achieve its science goal, CE needs to operate in a network with a minimum of two third-generation detectors, plus a third detector sensitive enough to be able to help localize the sources of interest. The CE Concept includes a 20 km detector to achieve this localization even for distant sources when running together with ET. As mentioned above, this 20 km detector has more challenging CTN requirements that the 40 km detector (see below).

Crucially, in the scenario where only one 40 km CE detector is built, for source localization that CE detector will have to rely heavily on upgraded second-generation partner observatories, such as LIGO India or LIGO Hanford or LIGO Livingston. Thus, for CE to be able to achieve its science goals, availability of low-thermal-noise and low-absorption optical coatings for detectors with shorter arms is even more essential, as 2nd generation detectors will have to be upgraded to help with source localization.

2.4 Study of the CE sensitivity for different coating designs

Figure 1 shows the impact of different CTN levels on the CE sensitivity, both for the 40 km and the 20 km detectors [7].

This study suggests that:

- Assuming the CE 40 km detector can run together with two other observatories with similar sensitivity, the baseline A+ coating thermal noise fully enables the CE science goals.
- However, improved coatings will be necessary to reach the 40 km detector facility limit, when quantum noise is also reduced beyond the baseline levels, or when the 40 km detector is tuned to maximize low frequency sensitivity.
- For CE 20 km, coatings better-than-A+ would already significantly improve astrophysics performance. Furthermore, the availability of coatings with lower than about A$^\sharp$ CTN level (4 times below Advanced LIGO level) would enable design changes that can reduce the cost of the CE 20 km facility.
- In the scenario where no 20 km detector is built, CE will have to rely on significantly shorter partner observatories, and coatings with CTN at least 4 times below A+ level ($0.5\times$"A$^\sharp$ CTN") would be highly desirable.
- If large scale optics with coatings at the A+ target level can not be achieved, then the astrophysical penalty will be appreciable in both the 40 km and 20 km detectors, but particularly in the 20 km one.

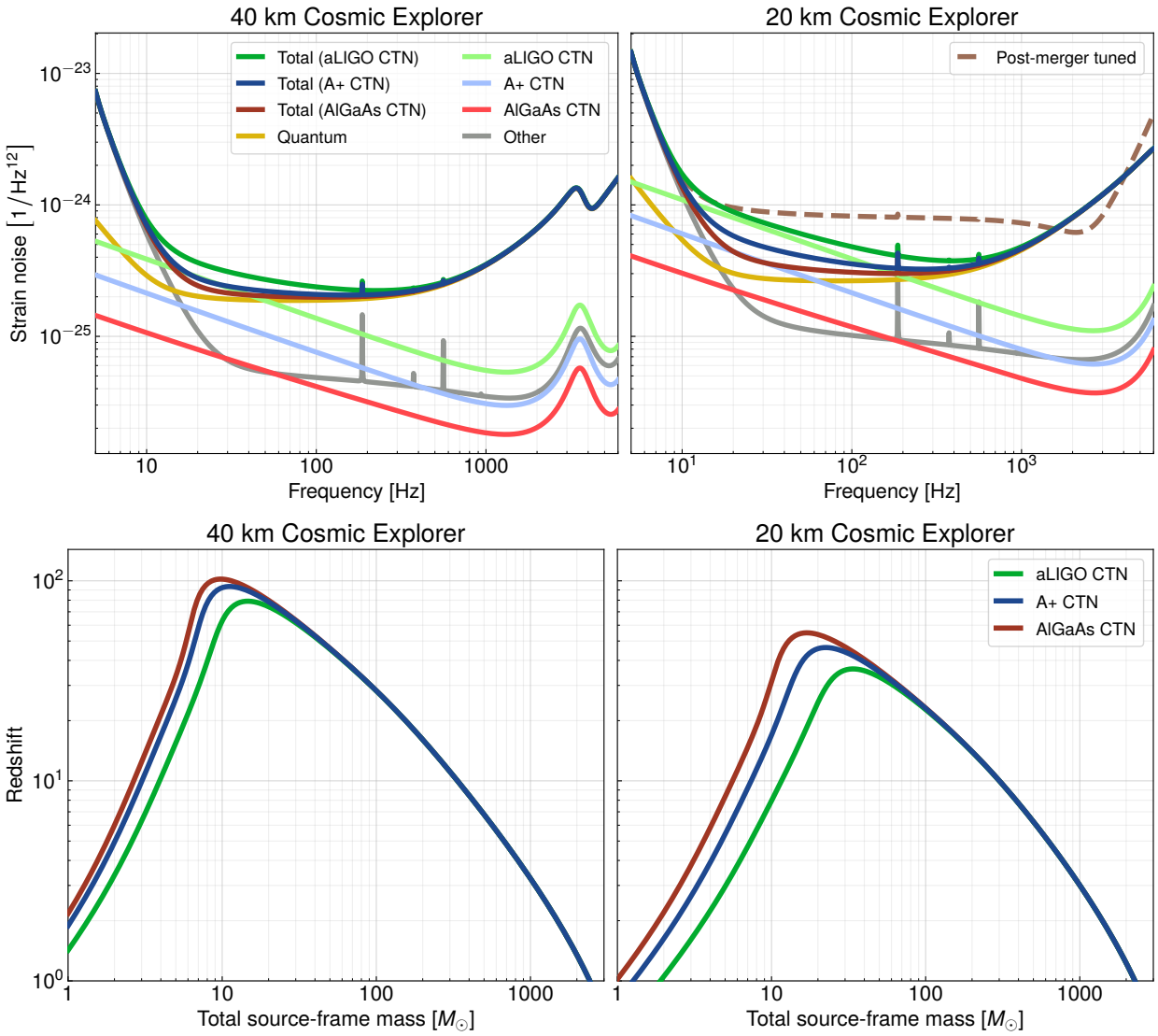

Figure 1: Upper two plots: Total noise and coating thermal noise of a $40\,\mathrm{km}$ CE (left) and a $20\,\mathrm{km}$ CE (minimal spot size - right), for different levels of coating thermal noise: Green: as measured by aLIGO witness samples (which is less than the observed noise in the current Advanced LIGO interferometer), Blue: A+ target level, Red: measured upper limit for AlGaAs coatings. Lower two plots: Resulting horizon redshift vs. total source frame mass $M_\odot$ for different levels of coating thermal noise.

2.5 Optical properties

2.5.1 Optical Absorption - Coating Absorption and Point Absorbers

Uniform Optical Absorption: Optical absorption in the interferometer test masses leads to thermal lensing and thus distortions of the optical surfaces. Advanced LIGO has test masses with coating absorptions around $0.5\,\mathrm{ppm}$ - the measured values of the 8 installed test masses are shown in Table 2. These values limited the Advanced LIGO arm powers to approximately $350\,\mathrm{kW}$.

Observatory	Optic	Serial No	Scatter ppm	Absorption ppm
LLO	ETMY	41	9.7	0.14
LLO	ETMX	42	7.4	0.32
LHO	ETMX	47	11	0.2
LHO	ETMY	50	8.2	0.21
LHO	ITMY	96	6.5	0.5
LLO	ITMX	98	10	0.4
LHO	ITMX	101	5.7	0.5
LLO	ITMY	102	14	0.3

Table 2: List of optical properties of optics currently installed in Advanced LIGO. Note that these are small-beam measurements taken outside the interferometer. In-situ optical absorption measurements for installed optics - using Hartman sensors, as well as changes in cavity g-factor - are consistent with a typical absorption around 0.5 ppm. Similarly, cavity round trip loss measurements suggest per-optic total losses between about 25 ppm and 35 ppm - most of that is some form of scatter. The excess compared to the table above is likely small-angle scatter that depends on the mirror surface large-scale structure. (Source: galaxy.ligo.caltech.edu/optics [8])

Thus simple power scaling suggests we should have less then about 0.17 ppm of optical absorption in the test mass coatings to achieve the full design arm power. Thus the research target should be about 0.1 ppm of absorption, which coincidentally is also a level that has been measured in selected coatings on small areas, making it a realistic goal.

Point Absorbers: Additionally, point absorbers on optical coatings - small $O(100\,\mu\text{m})$ diameter highly absorbing coating defects - have plagued Advanced LIGO, limiting the achievable operating arm power by distorting the arm cavity optics. Even spots with a total absorbed power around 10 mW are limiting [2, 9]. Additionally, optical distortions from point absorbers have a small spatial structure, making them very difficult to be compensated by mode control actuators [10].

One of the side effects of distorted test mass mirror surfaces is that higher order arm modes can also resonate light, modifying the optical response at offset frequencies corresponding to the mode's resonance condition. CE has the additional challenge that its cavity free spectral range is only slightly bigger than the observation band. Thus all effects from higher-order modes will end up in-band, and CE will be more sensitive to distorted optical surfaces.

While detailed modeling is still ongoing as part of the CE design work, initial analysis suggest that CE coatings need to have essentially zero point absorbers with mean radius of 12 µm or more across the whole beam spot, while some point absorbers of radius $< 5\,\mu\text{m}$ are acceptable [9].

In addition to wavefront distortions, thermal damage to the coatings is also of concern. Post-installation imaging on Advanced LIGO's amorphous coatings has revealed damage

around existing point absorbers, worsening their effect through exposure to high intensities. Similarly, Photothermal Common-Path Interferometer (PCI) absorption measurements have damaged AlGaAs coatings as well as amorphous Ti:Tanatala coatings (before LMA eliminated contamination point absorbers) at intensities of approximately $10\,\mathrm{kW/cm^2}$, similar to those anticipated in A♯. The damage occurred in a zipper-like pattern, initiated at a point absorber. Since one damage spot could render an entire mirror unusable, suitable optical coatings need to be able to handle intensities well in excess of $10\,\mathrm{kW/cm^2}$ to mitigate the risk of damaging coatings during testing and operation.

2.5.2 Coating Uniformity and Scale-Up

In addition to the absorption uniformity described above, the coating also need to fulfill a transmission uniformity requirement. A full analysis of the transmission uniformity requirement must be carried out for the CE optical coatings. However scaling from Advanced LIGO provides good initial estimates. To mitigate optical aberration from the mirror surfaces, the uniformity of the coatings will be required to be *circa* 0.1 % over at least 400 mm diameter. In addition to this, the mirrors in arm cavities will be required to have matching, defined as $2(T_1 - T_2)/(T_1 + T_2)$ to be around 5×10^{-3} or better. There is no demonstration of these requirements being met for ion beam deposition, or any other optical coating technology, to date. More generally there needs to be a scale-up in the ion beam deposition technology to enable optical coatings to be manufactured over 700 mm diameters. It is worth highlighting that other factors that drive inhomogeneity in the optical and mechanical properties could come into play, such as the difference in ion energy distribution as a function of the sputtering plume angle, or from the potential changes in deposition rate. The mechanisms that drive the inclusion of point absorbers and defects could also change, highlighting the need to de-risk and optimise the manufacturing processes.

2.5.3 Optical Scatter

Optical scattering on the end and input test masses is the biggest optical loss in the arm cavities. Indeed the interferometer is designed such that most of the power in the input laser ultimately gets lost through scatter in the arms. The specification for Advanced LIGO was 37.5 ppm per optics (75 ppm per arm round trip).

The Advanced LIGO interferometers achieve this specification: cavity round trip loss measurements suggest per-optic total losses between about 25 ppm and 35 ppm, most of which is some form of scatter. Power handling limitations are due not to this form of loss, rather to the optical absorption, which - despite only being a small fraction of the scatter loss - resulted in thermal aberrations and degraded interferometer performance, see section 2.5.1 above.

However, there are two primary reasons lower scatter is still desired: (i) scatter loss represents a significant fraction of the total optical loss in the squeezed light optical path, limiting the maximal amount of squeezing achievable in the readout, and (ii) the scattered light itself can reflect of walls and equipment in the vacuum chamber, and re-enter the interferometer as stray light. Thus optical scatter will drive the squeezed-light readout design and the arm baffling requirements.

2.5.4 Static and Induced Birefringence

Birefringence in the mirror coating and substrate can effect the gravitational-wave signal. Temporal fluctuations in the birefringence, which generate noise, can be caused by free body or modal oscillations of the mirror, or by fluctuations in thermal or stress conditions that produce strain-induced birefringence, or by audio-band fluctuations in the stray electric field. Additionally, spatial variations in birefringence can reduce the optical beam quality and introduce additional effective optical loses. They can be caused by gravity-induced stress, by uneven thermal heating, or by manufactuing defects.

Amorphous materials used in test mass mirrors contribute no significant birefringence. Fused silica is the material used for the mirror substrate and the low-index layer of amorphous mirror coatings. One can induce birefringence in fused silica, indeed the damped oscillations of stress-induced birefringence is used to measure the mechanical loss of this material. However the typical operating stress and temperature fluctuation experienced by the test mass mirrors do not induce significant birefringence. We therefore will focus the remainder of this discussion on crystalline materials, which are proposed solely for the mirror coatings, and specifically GaAs/AlGaAs mirror coatings. These GaAs/AlGaAs coatings — henceforth termed "AlGaAs coatings" — are currently the only crystalline coating being considered for CE.

The birefringence of an HR AlGaAs mirror coating will induce approximately 1 mrad phase difference at 1064 nm. Assuming that the polarization axes (crystal axes) of the ITM and ETM coatings are aligned, then the frequency separation of the cavity modes for s- and p-polarization is about 12 Hz for the LIGO 4 km detector and about 1.2 Hz for the CE 40 km detector. However, if the angle between the polarization axes is 90° then the splitting depends only on the difference in phase lag between the two mirrors, which is greatly reduced from the parallel axes configuration, though the variance in AlGaAs mirror birefringence has not been published to our knowledge. The orthogonal configuration, with a 90° offset in the crystal axes, minimizes, to second-order the total phase shift in the arm cavities [11].

$$\Delta\nu = \frac{\Delta\phi_i \pm \Delta\phi_e}{2\pi}\nu_{\mathrm{FSR}}, \quad \nu_{\mathrm{FSR}} = \frac{c}{2L} \quad \begin{cases} + & \text{if axes parallel} \\ - & \text{if axes perpendicular} \end{cases}$$

Michimura ([11]) requires that birefringence should produce a total optical loss as seen by the injected squeezed light of no more than 0.1 %. At this level the beam polarization and mirror crystal axes must be aligned to 1°. Free body motion of the test mass mirrors is minimal when the interferometer is locked. To achieve the birefringence noise limit, the roll mode motion, which has the largest coupling to birefringence noise, must be $< 10^{-10}$ rad/$\sqrt{\mathrm{Hz}}$ at 100 Hz. This limit is easily met as the allowed roll motion is $< 10^{-11}$ rad/$\sqrt{\mathrm{Hz}}$.[11].

Absorption in the mirror coating will generate a thermal profile in the coating. The thermal gradient will induce material strain and birefringence. While the thermal compensation system[10] is designed to minimize this thermal gradient, the residual gradient will induce a small, radially-dependent birefringence signal. Fluctuations in the thermal profile will there fore couple to birefringent noise.[12]

AlGaAs mirrors have a bandgap wavelength of 870 nm. The detector laser is at 1064 nm, which is below the bandgap energy, but two-photon interactions can excite some electrons

to the conduction band. As the absorption varies by depth in the coating, the free carriers will generate an electric field along the beam axis that alters the index via the electro-optic effect. Ma, et al.[13] studied the change in birefringence as a function of beam intensity (1550 nm) and exposure to above-bandgap light. They observed the shift in resonant frequency for a set of fixed cavities with AlGaAs mirrors operating at 4, 124, and 297 K. While the effect was clear, the magnitude of the frequency shift and change in birefringence is small: For their l=48 cm cavity, and of a beam intensities of I=10 kW/cm^2 the effect was on the order of

$$\frac{\Delta\nu}{\nu} = 5 \times 10^{-11}$$

towards a smaller line splitting. The effect is non-linear and saturates at higher powers, and was only measured as a slow drift - an experiment to measure transfer functions in the audio-band in being commissioned at Syracuse now. Nevertheless, if we assume the effect is linear at that magnitude, we find a phase response to intensity fluctuations on the order of

$$\Delta\phi = 2k\frac{\Delta\nu}{\nu}\frac{l}{I} \approx 3 \times 10^{-12}\,\frac{\mathrm{rad\,m^2}}{\mathrm{W}}$$

For Advanced LIGO and CE spot sizes respectively, this corresponds to an equivalent displacement per Watt of

$$\frac{\Delta x}{\Delta P} \approx 2 \times 10^{-17}\,\frac{\mathrm{m}}{\mathrm{W}}\,\text{(LIGO)}\ \text{ and }\ 5 \times 10^{-18}\,\frac{\mathrm{m}}{\mathrm{W}}\,\text{(CE)}$$

In addition, if the input and end test mass are chosen to have the polarization axes at 90° to each other, this effect would cancel to leading order.

For comparison, the f^{-2} radiation pressure coupling to the test masses at $f = 100$ Hz is

$$\frac{\Delta x_{\mathrm{RP}}}{\Delta P} \approx 4.2 \times 10^{-16}\,\frac{\mathrm{m}}{\mathrm{W}}\left(\frac{100\,\mathrm{Hz}}{f}\right)^2\,\text{(LIGO)}\ \text{ and }\ 5.3 \times 10^{-17}\,\frac{\mathrm{m}}{\mathrm{W}}\left(\frac{100\,\mathrm{Hz}}{f}\right)^2\,\text{(CE)}$$

and the f^{-1} photo-thermal coupling [14] of fused silica mirrors for $a = 1$ ppm absorption at $f = 100$ Hz is

$$\frac{\Delta x_{\mathrm{RP}}}{\Delta P} \approx 10^{-18}\,\frac{\mathrm{m}}{\mathrm{W}}\left(\frac{100\,\mathrm{Hz}}{f}\frac{a}{1\,\mathrm{ppm}}\right)\,\text{(LIGO)}\ \text{ and }\ 3 \times 10^{-19}\,\frac{\mathrm{m}}{\mathrm{W}}\left(\frac{100\,\mathrm{Hz}}{f}\frac{a}{1\,\mathrm{ppm}}\right)\,\text{(CE)}$$

At the moment, there is no evidence to suggest that any of the potential sources of birefringence noise is at a level that will impact the sensitivity of CE or A$^\sharp$. However, it is imperative that there be experimental verification of any upper limits on the noise. At Syracuse University there is an experiment led by Bin Wu that will test the birefringence noise induced by free carriers by observing the shift in the resonant frequency of a fixed cavity with AlGaAs end mirrors when exposed to light above the bandgap. In addition there are experiments at Syracuse University and Embry-Riddle that are designed to produce high resolution maps of the birefringence in AlGaAs coatings in a static state and under thermal and mechanical stresses. The Large Optic Crystalline Coating Characterization Instrument (LOCCCI) now being built at Syracuse will use an XY raster scan to map static and induced birefringence for large mirrors, including CE test mass mirrors.

3 Coating Solutions and Research Directions

This section of the document aims to capture mature coatings solutions for CE, as well as promising research directions which are still in the early stage of development.

3.1 Amorphous Coatings and Materials

Sustained research in amorphous coatings and materials is necessary to address the challenges that CE brings, in particular to support optical intensities > 10 kW/cm^2 without damage, to reduce absorption from 0.5 ppm to 0.1 ppm to support high arm power with acceptable figure distortion, and to further reduce thermal noise beyond the level currently achieved.

Optical damage in amorphous oxides are associated with point absorbers. The steps that LMA has taken for the current Ti:Ta2O5/SiO2 stacks to (largely) eliminate the metal inclusions due to flakes "shed" from the Grand Coater are not specific to a particular oxide material system, so should be applicable to any materials chosen for subsequent mirror designs. Verification that a modified Grand Coater at LMA (or another coater used for CE mirrors) has adequately low probability of metal inclusions that cause damage will be necessary; the research community can contribute damage characterization to coatings obtained from potential vendors. While there are not yet vendors with an IBS system large enough to support deposition of 70-cm coatings, efforts are underway to build that capability, with possible synergies with the high intensity laser community.

Absorption reduction is a familiar subject in the greater coating community, though levels below 0.5 ppm are rarely relevant, so are not much explored commercially. Typically, IR absorption in wide-bandgap oxides is not an intrinsic material property, but rather is associated with impurities or stoichiometric defects incorporated in the coating. While absorption cross-sections for various impurities can vary from host material to host material, they typically are broadly similar, so broadly speaking absorption at this level is, like damage threshold, addressable with largely material-independent methods. As an example, Rutherford backscattering measurements (RBS) on Ti:GeO2/SiO2 stacks identified the presence of 100 ppm molybdenum (sputtered from the control grids in the IBS system). Changing the Grand Coater over from Mo grids to Ti grids led to the production of mirrors by LMA with 0.5 – 0.6 ppm absorption, 3x lower than the best obtained with Mo grids. Ti:GeO2/SiO2 deposited with a Ti-grid IBS system at Strathclyde showed absorption as low as 0.2 ppm. The lowest absorption observed with LMA Ti:Ta2O5/SiO2 stacks are similar (0.2 ppm), though not consistently obtained at this level. A systematic approach to identifying impurities (and native defects) contributing to absorption in mirrors consisting of wide-bandgap oxides will be necessary to develop deposition/annealing strategies for their elimination.

To this point there is no evidence for phase noise on reflection from amorphous mirrors from sources other than the **thermal noise** resulting from mechanical losses in the coatings (other than thermo-elastic/optic noise which can be eliminated with appropriate mirror design). The lowest thermal noise predicted from single-layer loss measurements is at the 0.5 a-LIGO level for Ti:GeO2/SiO2 stacks. The lowest observed in direct thermal noise measurements is 0.6 a-LIGO. The difference between the noise predicted from single layer properties and that observed from a stack in this material system (and similar observations

in other material systems) exemplifies one of the challenges in developing low-noise coatings: empirical studies have brought to light complex process-dependent phenomena. There is no amorphous oxide material system at present with lower predicted thermal noise than the TiGeO2/SiO2 under development for A+LIGO. Theoretical and empirical exploration of alternatives such as high index heavy metal oxide dopants (like PbO), or incorporating network modifiers like MgO and ZnO, warrant investigation. Another direction for amorphous material studies is developing an understanding (and seeking reduction) of absorption in non-oxide silicon-based amorphous materials (SiNx, a-Si) which have adequately low mechanical losses but higher than acceptable optical absorption. Multi-materials coatings [15] remain an option if low-noise materials with somewhat too high optical absorption emerge. For shorter interferometers, the availability of large (30 cm diameter) wafers of high index wide bandgap crystalline wafers (SiC) can be explored as a 1-um version of the crystalline Si top layer(s) currently under investigation for 2-um applications). The investigation of new materials needs to happen in parallel with the exploration of new manufacturing methods/processes, such as heated deposition, alternative plasma assist technologies, alternative ion beam deposition configurations (plasma technology, ion energy, dep rate, uniformity optimisations through substrate motion etc, post-deposition heat treatment which could be key for materials that benefit from longer annealing and/or suffer from defect creation at higher temperatures e.g. blisters).

3.2 Crystalline AlGaAs Coatings

One of the advantages of AlGaAs coatings is that they are successfully being used as low thermal noise, low optical loss coatings in other precision optical experiments [16]. In these applications, AlGaAs coatings have demonstrated cavity finesse $> 400\,000$ [17], scatter $< 5\,\text{ppm}$ [18], optical absorption $< 1\,\text{ppm}$ [19], and uniformity better than $< 2\,\text{nm}$ over $5\,\text{cm}$ [20].

The primary challenge for developing AlGaAs coatings for interferometric gravitational wave detectors is to scale up the size of the coatings from the $\sim 1\,\mu\text{m} - 5\,\text{cm}$ diameters [16] typical of other applications to the $\geq 40\,-$cm diameter needed for future gravitational wave detectors. This development work is ongoing in the community. The construction processes divides into three steps, all of which need development to provide large AlGaAs coatings;

1. Acquisition of a gallium arsenide (GaAs) wafer with needed diameter,
2. Growth of AlGaAs coating on gallium arsenide wafer,
3. Bonding of AlGaAs coating onto test mass substrate.

For step 1, the largest GaAs wafers that are readily available commercially are $20\,-$cm in diameter. This limit existed due to lack of demand for larger sizes. However, as the market for more III-V based electronics grows, such as the current demand for Vertical Cavity Surface Emitting Lasers (VCSEL), the industry is exploring the transition to $30\,-$cm wafers to improve the economy of scale. In addition, a team of LIGO and CE researchers have already started work on a project to grow GaAs wafers on germanium (Ge) wafers. Ge wafers are currently available in $30\,-$cm diameters [21]. GaAs can be deposited on Ge at a rate of 100–300 µm/hr using Hydride Vapor Phase Epitaxy (HVPE). Thus a rough GaAs

wafer can be grown on the Ge wafer in a day. Once it is polished and the Ge etched away, the GaAs wafer is suitable for use in a molecular beam epitaxy (MBE) chamber for coating growth.

Step 2 involves the growth, via molecular beam epitaxy, of the AlGaAs mirror on the GaAs wafer. At present, research samples are grown at IQE [22]. Responding to industry demand, IQE has already retooled to be able to accommodate 30 −cm wafers. These chambers will need to be exceptionally clean and dedicated solely to production of CE mirrors to obtain the best optical properties [20, 23]. Bonders to make silicon-on-insulator wafers have been demonstrated up to 45 −cm diameter [24], but they can not take the thickness nor mass of the proposed gravitational wave detector optics. For step 3, a custom bonder is being developed to accommodate the larger size.

Research on oval defects and other potential scattering sources [25], the effects and possible noise from birefringence [26], and the cryogenic behavior of AlGaAs [27] is continuing. See this recent paper summarizing a recent workshop on AlGaAs [28] for more details on the current state of AlGaAs coatings for gravitational wave detectors.

3.3 Early High risk-High reward research: metasurfaces

Bragg reflectors require dozens of layers of alternating high and low index of refraction to produce high levels of reflectivity, and current research for reducing CTN is focused on finding materials with lower mechanical loss. Alternative approaches exist to achieve the same reflectivity with much lower CTN by reducing the thickness of the mirror, for example a sub-wavelength structured surface (or metasurface), in combination with a much reduced Bragg stack.

Metasurfaces are arrays of sub-wavelength spaced periodic nanostructures that offer a novel approach to manipulating light-matter interactions with local resonances [29]. They hold promise for reducing CTN due to being only a few hundred nanometers thick, compared to several micrometres for a Bragg stack. The highest reflectivity achieved with a metamaterial mirror is 99.8 % [30], and thus to achieve the required levels for the test masses one would need to combine the metamaterial with a Bragg stack of a few layers. This concept has been explored to produce mirrors at a wavelength of 1550 nm using an etching process [31, 32, 33], which leads to high surface roughness. Investigation is needed into the fabrication of such mirrors at a wavelength of 1064 nm using atomic layer deposition, which leads to extremely smooth structures [34], thus reducing scattering loss.

This approach is still at the early stages of design and fabrication, and while it could lead to significant CTN reduction, there are further challenges involved for implementation in gravitational wave detectors. Scatter and absorption losses need to be minimized using various nanofabrication techniques. If a viable candidate design is found for the mirrors, the next steps would involve scaling up the fabrication to test mass size and testing the mirror at high power levels.

4 Metrology

4.1 Metrology for optical properties

Accurate metrology of the CE test mass is needed to characterize, absorption, uniformity, scatter and birefringence.

For all potential technologies for CE, the scale-up of the optical coatings over large area is a key challenge. Relevant manufacturing technologies, such as ion beam deposition, must be developed that can reach the uniformity requirements over large area. The international CE consortium must ensure that the factors that drive defects and inhomogeneities, within the manufacture, are suitably understood and mitigated. Testbeds must be developed to allow characterization of mirror figure, transmission, reflection, absorption, birefringence and scatter, over 700 mm diameters.

For crystalline coatings like AlGaAs, it is important to characterize the level of birefringence and birefringence non-uniformity. Uniform birefringence is less worrisome than non-uniform birefringence because the fast axis can be aligned with the optical polarization. Non-uniform birefringence can not be easily canceled by test-mass rotation and acts as a source of optical loss similar to scatter from surface figure imperfections. Phase non-uniformity imparted by birefringence can be directly compared to the phase non-uniformity imparted by figure deviations. Ongoing measurements at Embry-Riddle, show birefringence amplitude variations of ~ 0.2 mrad over millimeter distances. This is equivalent to 0.02 nm surface figure variations, which is about $1/10^{\text{th}}$ of the rms figure variation in a typical aLIGO test mass surface (after removing abberations Z1-4) [8]. Since the test masses appear to have scatter losses of around 30 ppm (see caption to Table 2) we can infer that the optical losses from birefringence fluctuation will be "a few" ppm. As we scale to larger coatings, we will need to ensure that the optical loss due to birefringence non-uniformity remains smaller than optical loss due to other sources. The LOCCCI instrument being built at Syracuse University will allow us to make birefringence maps on full-sized optics and estimate the associated optical loss. Characterization of smaller test/witness samples will continue at Embry-Riddle where a resonant-cavity based version of the mapping instrument is being built that will significantly improve birefringence mapping sensitivity and spatial resolution.

Coatings whose layer materials have a large thermo-optic coefficient (index change with temperature) may have a special layer structure design that minimizes thermo-optic noise. We refer to such coatings as "thermo-optically optimized". AlGaAs coatings in particular must be thermo-optically optimized so that thermo-optic noise is not a significant portion of the overall noise budget. Obtaining high level of noise reduction by this method requires good knowledge of the layer material indices, expansion coefficients, thermo-optic coefficients, and good control over the layer thicknesses. The thermo-optic response of optimized coatings should therefore be checked directly as the coating size is increased. Instruments for this purpose are currently available at Embry-Riddle and Urbino University. Samples up to 10 cm in diameter can currently be accommodated, but the instruments could be scaled up to accommodate larger samples.

As mentioned earlier, both crystalline and amorphous coatings have been damaged by intensities comparable to those proposed for CE. Therefore, it will be useful to obtain instruments

capable of making *non-destructive* measurements of the laser damage threshold for specific individual mirrors. Such an instrument would presumably consist of scanning a coating with an increasingly high intensity beam while monitoring the temperature with a thermal camera. Extrapolation to the break-down temperature (previously measured on sacrificial samples) gives an estimate of the laser damage threshold of the specific mirror in question. Such an instrument does not currently exist but would be constructed within the collaboration.

As previously noted, the number of point-aborbers in current IBS coatings will need to be reduced if we are to produce coatings for several test masses with zero point defects over the 70 cm area of a CE mirror. This is also true for AlGaAs coatings. The number of point-defects in AlGaAs coatings has been going down as the technology improves. For example, between 2017 and 2023, the number of defects went from order 100 defects/cm^2 to order 1 defect/cm^2 [35]. As in the case of IBS coatings, defects in AlGaAs arise from the introduction of contaminants onto the coating surface during the growth process, possibly from gallium spitting. Similarly, reduction of background absorption requires improved cleanliness of the growth environment. Therefore, the collaboration will need access to an MBE facility that can be dedicated growth of large-area, low-absorption coatings for an extended period.

4.2 Metrology for coating thermal noise

Measurements of the CTN for test samples can be either done directly or indirectly via the Fluctuation-Dissipation Theorem by measuring mechanical dissipation.

Direct measurements are essential for CTN verification, but also challenging as they need to be done in the audio-band in laboratory environments that vibrate a lot more than the mirror coating thermal noise. The LIGO-MIT thermal noise experiment exploits the different coupling of thermal noise to the TEM20 and TEM02 optical modes [1]. This experiment will be upgraded with AlGaAs auxiliary mirrors, as the thermal noise from the amorphous auxiliary mirrors limits the sensitivity. The data requires some level of interpretation, as it is sensitive to the difference in TEM20 and TEM02 thermal noise for a relatively small spot size. A version of this experiment able to directly probe the LIGO test masses is under development. This direct approach of measuring thermal noise has a relatively slow turn-around time, a gap the indirect measurements can fill.

Indirect methods measure the ring-down of optical samples to infer their dissipation, and thus their CTN. The fastest turn-around setup that also works well for coated disc samples is the GENS geometry [36], balancing the test sample on a lens to minimize suspension losses. There are multiple GENS apparatuses available across the research community (including at Caltech and Syracuse). One of the Syracuse units is able to also measure coating losses down to 10 K.

5 Timeline for Coatings Research

The fundamental research required to improve optical coatings by its nature tends to be difficult to ramp up rapidly on demand. Thus, the time scales on which coatings improvements can significantly impact the future of terrestrial GW detectors is important to guide the research. At least four different time scales exist:

A$^\sharp$ Optics Installation (∼2028): The Advanced LIGO O5 observation run is expected to last until 2028. After that, the A$^\sharp$ detector upgrade can extend Advanced LIGO's range to observe the first binary merger at the time of peak star formation, and test significant aspects of the the technology for CE, including upgraded coating options.

Impact on CE Design (∼2029): Breakthrough reductions in optical coating absorptions and (for the 20 km detector) the coating thermal noise have the potential to simplify the CE design. The deadline for such design simplification is the Preliminary Design Review for CE, which is anticipated towards the end of the 2020s.

CE optic manufacturing (mid-2030s): The construction of CE is anticipated to happen during the first half of the 2030s. The optics need to be installed towards the end of construction, but will likely require a year or two for manufacturing, polishing and coating.

CE Upgrades (post-2040): CE is envisioned as a detector facility that can house multiple generations of detectors. Much like in Advanced LIGO, upgrading the CE optics will remain an option should significant coating improvements become available.

6 Research and Development Recommendations

Based on the analysis and discussion in the previous sections, the path forward for coating development for CE can be summarized as follows:

- The long arm and associated large beam size makes the CE 40 km detector less sensitive to CTN than any other proposed terrestrial GW detector concept (see Table 1), allowing it to achieve unmatched cosmological reach even with current coating technology. However...
- ... achieving the A+ coating target is required for CE to reach its design sensitivity. Not achieving the A+ coating target could result in a significant penalty in CE astrophysical output, especially for the 20 km detector.
- Achieving low coating optical absorption and coatings with zero significant point-absorbers is equally important for CE to achieve its operating arm power. Realizing 0.1 ppm of optical absorption in all test mass coatings would significantly simplify the CE design and operations, and reduce the project risk associated with thermal aberrations.
- Improvements beyond the A+ coating thermal noise design target are beneficial for a 20 km detector, while in a 40 km detector the benefit will be achieved once quantum noise is also reduced, to reach the facility limit.
- Improvements by at least a factor of two beyond the A+ design coating thermal noise and beyond current optical absorption levels are *essential* for shorter partner observatories, on which some CE science will rely if the 20 km detector is not built.

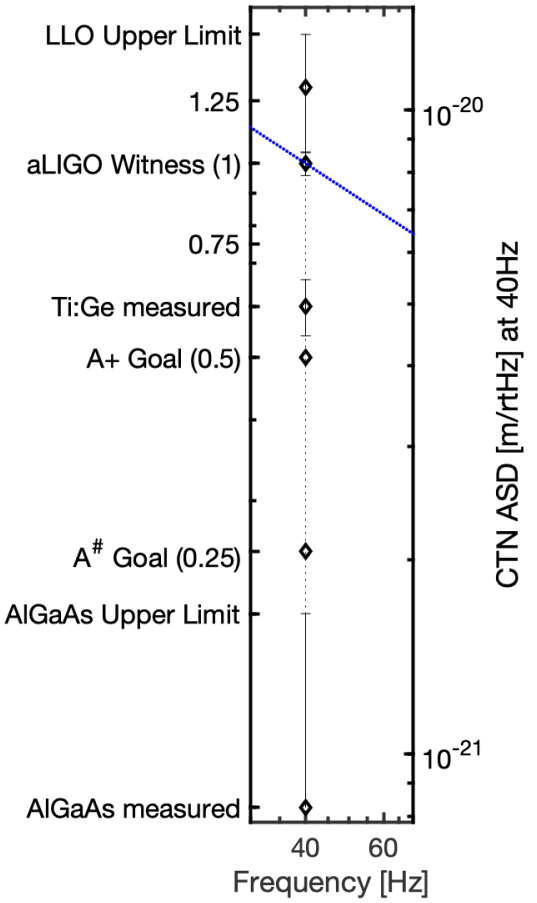

Figure 2: Coating Thermal Noise (CTN) of measured coating samples, and research goals. Left axis: scaled to the aLIGO witness sample coatings. Right: Thermal noise at 40 Hz for LIGO spot size and arm length - see Table 1 for CTN scaling to CE observatories. Blue line: measured frequency dependence of coating thermal noise (a power law of 0.45). ([1, 37])

- Improvements by a factor of two beyond the A+ design coating thermal noise may also result in a overall cost reduction for 20 km detector by allowing for smaller optics.

To maximize the CE scientific output, it is therefore important:

- To continue research in amorphous materials and improve upon the existing Advanced LIGO coatings to meet or exceed the A+ goals, and to lower optical absorption.
- To explore materials which have the potential to go beyond the A+ coating targets, as a possible future upgrade to bring the CE sensitivity close to the limits imposed by the new facilities. These coatings will be especially important for shorter partner observatories (e.g., in existing facilities) if a 20 km CE is not built.
- To further characterize and improve the optical properties and manufacturability of AlGaAs crystalline coatings, currently the only coating material that has demonstrated a thermal noise low enough for all future detectors (CE and A$^\sharp$).
- To understand the discrepancy between best-fit observed $f^{-.45}$ in Advanced LIGO and the aLIGO CTN measured in witness samples.

A Coating Parameters and Scaling Laws

CTN scales, in amplitude, as $(L_{\rm arm} \times w)^{-1}$, where $L_{\rm arm}$ is the arm length, and w is the beam radius size. For a fixed cavity geometry, the beam size scales as $w \propto \sqrt{L_{\rm arm}}$, thus CTN scales overall as $L_{\rm arm}^{-3/2}$ [38]. For this reason, the longer the interferometer arm, the lower the thermal noise – with the caveat that the mirror size needs to increase to accommodate the larger beam spot.

Parameter	**Units**	**A+**	**AlGaAs**
High Index Layers			
Loss angle		9.0×10^{-5}	6.2×10^{-6}
Refractive index		2.09	2.09
Young's modulus	GPa	120	120
Poisson ratio		0.29	0.29
Thermal conductivity	W/m/K	33	33
Thermal expansion coeff.	ppm/K	3.6	3.6
Thermorefractive coeff.	ppm/K	14	14
Heat capacity per volume	J/K/m^3	2.1×10^6	2.1×10^6
Low Index Layers			
Loss angle		1.3×10^{-5}	6.2×10^{-6}
Refractive index		1.45	1.45
Young's modulus	GPa	70	70
Poisson ratio		0.19	0.19
Thermal conductivity	W/m/K	1.38	1.38
Thermal expansion coeff.	ppm/K	0.51	0.51
Thermorefractive coeff.	ppm/K	8	8
Heat capacity per volume	J/K/m^3	1.6×10^6	1.6×10^6

Table 3: Coating parameters used to calculate coating thermal noise in [5]. The AlGaAs loss angles are reverse-engineered to produce the upper limit for AlGaAs coating thermal noise measured in LIGO-G2001592. As such, and since a coating design canceling thermo-optic noise does not yet exist for these coatings, the coating Brownian noise calculated with these loss angles is taken as the total coating thermal noise for the AlGaAs coatings in this report.

References

[1] S. Gras, H. Yu, W. Yam, D. Martynov, and M. Evans. Audio-band coating thermal noise measurement for advanced ligo with a multimode optical resonator. *Phys. Rev. D*, 95:022001, Jan 2017. URL: https://link.aps.org/doi/10.1103/PhysRevD.95.022001, doi:10.1103/PhysRevD.95.022001.

[2] Aidan F. Brooks et al. Point absorbers in advanced ligo. *Applied Optics*, 60(13):4047, April 2021. URL: http://dx.doi.org/10.1364/AO.419689, doi:10.1364/ao.419689.

[3] Craig Cahillane. Ultra-High Power Photoneutralization Cavity for Neutral Beam Injection in Fusion Reactors, 2024. URL: https://arpa-e.energy.gov/technologies/projects/ultra-high-power-photoneutralization-cavity-neutral-beam-injection-fusion.

[4] Matthew Evans, Rana X Adhikari, Chaitanya Afle, Stefan W. Ballmer, Sylvia Biscoveanu, Ssohrab Borhanian, Duncan A. Brown, Yanbei Chen, Robert Eisenstein, Alexandra Gruson, Anuradha Gupta, Evan D. Hall, Rachael Huxford, Brittany Kamai, Rahul Kashyap, Jeff S. Kissel, Kevin Kuns, Philippe Landry, Amber Lenon, Geoffrey Lovelace, Lee McCuller, Ken K. Y. Ng, Alexander H. Nitz, Jocelyn Read, B. S. Sathyaprakash, David H. Shoemaker, Bram J. J. Slagmolen, Joshua R. Smith, Varun Srivastava, Ling Sun, Salvatore Vitale, and Rainer Weiss. A horizon study for Cosmic Explorer: Science, observatories, and community, 2021. arXiv:2109.09882.

[5] Peter Fritschel, Kevin Kuns, et al. Report of the LSC Post-O5 Study Group. Technical Report LIGO-T2200287, LIGO Scientific Collaboration, 2022. URL: https://dcc.ligo.org/LIGO-T2200287.

[6] GariLynn Billingsley. AlGaAs Coating Development Status for NSF September 2024. Technical Report LIGO-G2401659, LIGO, 2024. URL: https://dcc.ligo.org/LIGO-G2401659.

[7] Kevin Kuns. Impact of Coatings on the Cosmic Explorer Sensitivity. Technical Report CE-G2400028, CE, 2024. URL: https://dcc.cosmicexplorer.org/CE-G2400028.

[8] GariLynn Billingsley. LIGO Optics Summary Page (Galaxy page). Technical Report https://galaxy.ligo.caltech.edu/optics/, LIGO. URL: https://galaxy.ligo.caltech.edu/optics/.

[9] Wenxuan Jia, Hiroaki Yamamoto, Kevin Kuns, Anamaria Effler, Matthew Evans, Peter Fritschel, R. Abbott, C. Adams, R. X. Adhikari, A. Ananyeva, S. Appert, K. Arai, J. S. Areeda, Y. Asali, S. M. Aston, C. Austin, A. M. Baer, M. Ball, S. W. Ballmer, S. Banagiri, D. Barker, L. Barsotti, J. Bartlett, B. K. Berger, J. Betzwieser, D. Bhattacharjee, G. Billingsley, S. Biscans, C. D. Blair, R. M. Blair, N. Bode, P. Booker, R. Bork, A. Bramley, A. F. Brooks, D. D. Brown, A. Buikema, C. Cahillane, K. C. Cannon, X. Chen, A. A. Ciobanu, F. Clara, C. M. Compton, S. J. Cooper, K. R. Corley, S. T. Countryman, P. B. Covas, D. C. Coyne, L. E. H. Datrier, D. Davis, C. Di Fronzo, K. L. Dooley, J. C. Driggers, P. Dupej, S. E. Dwyer, T. Etzel, T. M. Evans, J. Feicht, A. Fernandez-Galiana, V. V. Frolov, P. Fulda, M. Fyffe, J. A. Giaime, K. D. Giardina, P. Godwin, E. Goetz, S. Gras, C. Gray, R. Gray, A. C. Green,

E. K. Gustafson, R. Gustafson, E. D. Hall, J. Hanks, J. Hanson, T. Hardwick, R. K. Hasskew, M. C. Heintze, A. F. Helmling-Cornell, N. A. Holland, J. D. Jones, S. Kandhasamy, S. Karki, M. Kasprzack, K. Kawabe, N. Kijbunchoo, P. J. King, J. S. Kissel, Rahul Kumar, M. Landry, B. B. Lane, B. Lantz, M. Laxen, Y. K. Lecoeuche, J. Leviton, J. Liu, M. Lormand, A. P. Lundgren, R. Macas, M. MacInnis, D. M. Macleod, G. L. Mansell, S. Márka, Z. Márka, D. V. Martynov, K. Mason, T. J. Massinger, F. Matichard, N. Mavalvala, R. McCarthy, D. E. McClelland, S. McCormick, L. McCuller, J. McIver, T. McRae, G. Mendell, K. Merfeld, E. L. Merilh, F. Meylahn, T. Mistry, R. Mittleman, G. Moreno, C. M. Mow-Lowry, S. Mozzon, A. Mullavey, T. J. N. Nelson, P. Nguyen, L. K. Nuttall, J. Oberling, Richard J. Oram, C. Osthelder, D. J. Ottaway, H. Overmier, J. R. Palamos, W. Parker, E. Payne, A. Pele, R. Penhorwood, C. J. Perez, M. Pirello, H. Radkins, K. E. Ramirez, J. W. Richardson, K. Riles, N. A. Robertson, J. G. Rollins, C. L. Romel, J. H. Romie, M. P. Ross, K. Ryan, T. Sadecki, E. J. Sanchez, L. E. Sanchez, T. R. Saravanan, R. L. Savage, D. Schaetzl, R. Schnabel, R. M. S. Schofield, E. Schwartz, D. Sellers, T. Shaffer, D. Sigg, B. J. J. Slagmolen, J. R. Smith, S. Soni, B. Sorazu, A. P. Spencer, K. A. Strain, L. Sun, M. J. Szczepańczyk, M. Thomas, P. Thomas, K. A. Thorne, K. Toland, C. I. Torrie, G. Traylor, M. Tse, A. L. Urban, G. Vajente, G. Valdes, D. C. VanderHyde, P. J. Veitch, K. Venkateswara, G. Venugopalan, A. D. Viets, T. Vo, C. Vorvick, M. Wade, R. L. Ward, J. Warner, B. Weaver, R. Weiss, C. Whittle, B. Willke, C. C. Wipf, L. Xiao, Hang Yu, Haocun Yu, L. Zhang, M. E. Zucker, and J. Zweizig. Point absorber limits to future gravitational-wave detectors. *Phys. Rev. Lett.*, 127:241102, Dec 2021. URL: https://link.aps.org/doi/10.1103/PhysRevLett.127.241102, doi:10.1103/PhysRevLett.127.241102.

[10] Jonathan Richardson. Next-Gen Thermal Compensation Technology. Technical Report LIGO-G2401284, LIGO, 2024. URL: https://dcc.ligo.org/LIGO-G2401284.

[11] Yuta Michimura, Haoyu Wang, Francisco Salces-Carcoba, Christopher Wipf, Aidan Brooks, Koji Arai, and Rana X. Adhikari. Effects of mirror birefringence and its fluctuations to laser interferometric gravitational wave detectors. *Physical Review D*, 109(2), January 2024. URL: http://dx.doi.org/10.1103/PhysRevD.109.022009, doi:10.1103/physrevd.109.022009.

[12] Yu-Pei Zhang, Shi-Xiang Yang, Wen-Hai Tan, Cheng-Gang Shao, Yiqiu Ma, and Shan-Qing Yang. Brownian thermal birefringent noise due to non-diagonal anisotropic photoelastic effect in multilayer coated mirrors, 2024. URL: https://arxiv.org/abs/2407.01634, arXiv:2407.01634.

[13] C. Y. Ma, J. Yu, T. Legero, S. Herbers, D. Nicolodi, M. Kempkes, F. Riehle, D. Kedar, J. M. Robinson, J. Ye, and U. Sterr. Ultrastable lasers: investigations of crystalline mirrors and closed cycle cooling at 124 k, 2024. URL: https://arxiv.org/abs/2404.02647, arXiv:2404.02647.

[14] Stefan W. Ballmer. Photothermal transfer function of dielectric mirrors for precision measurements. *Physical Review D*, 91(2), January 2015. URL: http://dx.doi.org/10.1103/PhysRevD.91.023010, doi:10.1103/physrevd.91.023010.

[15] William Yam, Slawek Gras, and Matthew Evans. Multimaterial coatings with reduced thermal noise. *Phys. Rev. D*, 91:042002, Feb 2015. URL: https://link.aps.org/doi/10.1103/PhysRevD.91.042002, doi:10.1103/PhysRevD.91.042002.

[16] Gregory Harry, Tim P Bodiya, and Riccardo DeSalvo. *Optical Coatings and Thermal Noise in Precision Measurement*. Cambridge University Press, 2012.

[17] Gar-Wing Truong, Lukas W. Perner, D. Michelle Bailey, Georg Winkler, Seth B. Cataño-Lopez, Valentin J. Wittwer, Thomas Südmeyer, Catherine Nguyen, David Follman, Adam J. Fleisher, Oliver H. Heckl, and Garrett D. Cole. Transmission-dominated mid-infrared supermirrors with finesse exceeding 400,000. *Nature*, 14(7846), 2020. URL: https://rdcu.be/dUsH1.

[18] G. Winkler, L. W. Perner, G.-W. Truong, G. Zhao, D. Bachmann, A. S. Mayer, J. Fellinger, D. Follman, P. Heu, C. Deutsch, D. M. Bailey, H. Peelaers, S. Puchegger, A. J. Fleisher, G. D. Cole, and O. H. Heckl. Mid-infrared interference coatings with excess optical loss below 10 ppm. *Optica*, 8(5):686–696, May 2021. URL: https://opg.optica.org/optica/abstract.cfm?URI=optica-8-5-686, doi:10.1364/OPTICA.405938.

[19] Manuel Marchiò, Raffaele Flaminio, Laurent Pinard, Daniéle Forest, Christoph Deutsch, Paula Heu, David Follman, and Garrett D. Cole. Optical performance of large-area crystalline coatings. *Opt. Express*, 26(5):6114–6125, Mar 2018. URL: https://opg.optica.org/oe/abstract.cfm?URI=oe-26-5-6114, doi:10.1364/OE.26.006114.

[20] P. Koch, G. D. Cole, C. Deutsch, D. Follman, P. Heu, M. Kinley-Hanlon, R. Kirchhoff, S. Leavey, J. Lehmann, P. Oppermann, A. K. Rai, Z. Tornasi, J. Wöhler, D. S. Wu, T. Zederbauer, and H Lück. Thickness uniformity measurements and damage threshold tests of large-area gaas/algaas crystalline coatings for precision interferometry. *Opt. Express*, 27(25):36731–36740, Dec 2019. URL: https://opg.optica.org/oe/abstract.cfm?URI=oe-27-25-36731, doi:10.1364/OE.27.036731.

[21] Umicore. Germanium substrates. URL: https://eom.umicore.com/en/germanium-solutions/products/germanium-substrates/.

[22] IQE. Our core technology. URL: https://www.iqep.com/innovation/our-core-technology/.

[23] Garrett D. Cole, Wei Zhang, Bryce J. Bjork, David Follman, Paula Heu, Christoph Deutsch, Lindsay Sonderhouse, John Robinson, Chris Franz, Alexei Alexandrovski, Mark Notcutt, Oliver H. Heckl, Jun Ye, and Markus Aspelmeyer. High-performance near- and mid-infrared crystalline coatings. *Optica*, 3(6):647–656, Jun 2016. URL: https://opg.optica.org/optica/abstract.cfm?URI=optica-3-6-647, doi:10.1364/OPTICA.3.000647.

[24] Dylan McGrath. EV Group to ship 450-mm wafer bonding tool, 2011. URL: https://www.eetimes.com/ev-group-to-ship-450-mm-wafer-bonding-tool/.

[25] K. Regiński J Kaniewski K. Klíma, M. Kaniewska. Oval defects in the MBE grown AlGaAs/InGaAs/GaAs and InGaAs/GaAs structures. *Crystal Research and Technology*, 34(5):683–687, 1999. URL: https://onlinelibrary.wiley.com/doi/10.

1002/(SICI)1521-4079(199906)34:5/6%3C683::AID-CRAT683%3E3.0.CO;2-T, doi:10.1002/(sici)1521-4079(199906)34:5/6<683::aid-crat683>3.0.co;2-t.

[26] Giuseppe Leo, Gaetano Assanto, Olivier Durand, and Vincent Berger. Characterization of AlGaAs/AlAs waveguides for optical parametric interactions. *J. Opt. Soc. Am. B*, 19(4):902–910, Apr 2002. URL: https://opg.optica.org/josab/abstract.cfm?URI=josab-19-4-902, doi:10.1364/JOSAB.19.000902.

[27] Dhruv Kedar, Jialiang Yu, Eric Oelker, Alexander Staron, William R. Milner, John M. Robinson, Thomas Legero, Fritz Riehle, Uwe Sterr, and Jun Ye. Frequency stability of cryogenic silicon cavities with semiconductor crystalline coatings. *Optica*, 10(4):464–470, Apr 2023. URL: https://opg.optica.org/optica/abstract.cfm?URI=optica-10-4-464, doi:10.1364/OPTICA.479462.

[28] Garrett D. Cole, S. W. Ballmer, G. Billingsley, S. B. Cataño-Lopez, M. Fejer, P. Fritschel, A. M. Gretarsson, G. M. Harry, D. Kedar, T. Legero, C. Makarem, S. D. Penn, D. H. Reitze, J. Steinlechner, U. Sterr, S. Tanioka, G.-W. Truong, J. Ye, and J. Yu. Substrate-transferred GaAs/AlGaAs crystalline coatings for gravitational-wave detectors. *Applied Physics Letters*, 122(110502), 2022. URL: https://doi.org/10.1063/5.0140663.

[29] Mohammadreza Khorasaninejad, Wei Ting Chen, Robert Charles Devlin, Jaewon Oh, Alexander Y. Zhu, and Federico Capasso. Metalenses at visible wavelengths: Diffraction-limited focusing and subwavelength resolution imaging. *Science*, 352:1190 – 1194, 2016. URL: https://api.semanticscholar.org/CorpusID:16455445.

[30] Stefanie Kroker, Thomas Käsebier, Stefan Steiner, Ernst-Bernhard Kley, and Andreas Tünnermann. High efficiency two-dimensional grating reflectors with angularly tunable polarization efficiency. *Applied Physics Letters*, 102(16):161111, April 2013. doi:10.1063/1.4802883.

[31] Johannes Dickmann and Stefanie Kroker. Highly reflective low-noise etalon-based metamirror. *Phys. Rev. D*, 98:082003, Oct 2018. URL: https://link.aps.org/doi/10.1103/PhysRevD.98.082003, doi:10.1103/PhysRevD.98.082003.

[32] Marcus Ossiander, Maryna Leonidivna Meretska, Sarah Rourke, Christina Spägele, Xinghui Yin, Ileana-Cristina Benea-Chelmus, and Federico Capasso. Metasurface-stabilized optical microcavities. *Nature Communications*, 14, 2022. URL: https://api.semanticscholar.org/CorpusID:251564396.

[33] Johannes Dickmann, Steffen Sauer, Jan Meyer, Mika Gaedtke, Thomas Siefke, Uwe Brückner, Jonathan Plentz, and Stefanie Kroker. Experimental realization of a 12,000-finesse laser cavity based on a low-noise microstructured mirror. *Communications Physics*, 6:16, 01 2023. doi:10.1038/s42005-023-01131-1.

[34] Robert C. Devlin, Mohammadreza Khorasaninejad, Wei Ting Chen, Jaewon Oh, and Federico Capasso. Broadband high-efficiency dielectric metasurfaces for the visible spectrum. *Proceedings of the National Academy of Sciences*, 113(38):10473–10478, 2016. URL: https://www.pnas.org/doi/abs/10.1073/pnas.1611740113, arXiv:https://www.pnas.org/doi/pdf/10.1073/pnas.1611740113, doi:10.1073/pnas.1611740113.

[35] Andri Gretarsson, Steve Penn, Gregg Harry, Garrett Cole, Ellie Gretarsson, and Breck Meagher. Algaas status. URL: https://dcc.ligo.org/DocDB/0190/G2301952/.

[36] Elisabetta Cesarini, Matteo Lorenzini, Gianpietro Cagnoli, and Francesco Piergiovanni. A gentle nodal suspension for measurements of the acoustic attenuation in materials. In *2014 IEEE Metrology for Aerospace (MetroAeroSpace)*, pages 528–532, 2014. doi:10.1109/MetroAeroSpace.2014.6865982.

[37] Valery Frolov. LLO alog DARM excess noise. URL: https://alog.ligo-la.caltech.edu/aLOG/index.php?callRep=70274.

[38] B P Abbott et al. Exploring the sensitivity of next generation gravitational wave detectors. *Classical and Quantum Gravity*, 34(4):044001, jan 2017. URL: https://dx.doi.org/10.1088/1361-6382/aa51f4, doi:10.1088/1361-6382/aa51f4.